



**Providing Choice & Value**

Generic CT and MRI Contrast Agents



CONTACT REP

**AJNR**

**White Matter Reorganization After Surgical Resection of Brain Tumors and Vascular Malformations**

M. Lazar, A.L. Alexander, P.J. Thottakara, B. Badie and A.S. Field

This information is current as of July 31, 2025.

*AJNR Am J Neuroradiol* 2006, 27 (6) 1258-1271  
<http://www.ajnr.org/content/27/6/1258>

**ORIGINAL  
RESEARCH**

M. Lazar  
A.L. Alexander  
P.J. Thottakara  
B. Badie  
A.S. Field

# White Matter Reorganization After Surgical Resection of Brain Tumors and Vascular Malformations

**BACKGROUND AND PURPOSE:** Diffusion tensor imaging (DTI) and white matter tractography (WMT) are promising techniques for estimating the course, extent, and connectivity patterns of the white matter (WM) structures in the human brain. In this study, DTI and WMT were used to evaluate WM tract reorganization after the surgical resection of brain tumors and vascular malformations.

**METHODS:** Pre- and postoperative DTI data were obtained in 6 patients undergoing surgical resection of brain lesions. WMT using a tensor deflection algorithm was used to reconstruct WM tracts adjacent to the lesions. Reconstructed tracts included corticospinal tracts, the corona radiata, superior longitudinal and inferior fronto-occipital fasciculi, cingulum bundles, and the corpus callosum.

**RESULTS:** WMT revealed a series of tract alteration patterns including deviation, deformation, infiltration, and apparent tract interruption. In general, the organization of WM tracts appeared more similar to normal anatomy after resection, with either disappearance or reduction of the deviation, deformation, or infiltration present preoperatively. In patients whose lesions were associated with corticospinal tract involvement, the WMT reconstructions showed that the tract was preserved during surgery and improved in position and appearance, and this finding correlated with improvement or preservation of motor function as determined by clinical assessment.

**CONCLUSION:** WMT is useful for appreciating the complex relationships between specific WM structures and the anatomic distortions created by brain lesions. Further studies with intraoperative correlation are necessary to confirm these initial findings and to determine WMT utility for presurgical planning and evaluation of surgical treatments.

White matter tractography (WMT) is a noninvasive technique used for in vivo visualization of white matter (WM) structures in the human brain.<sup>1-5</sup> It is based on diffusion tensor imaging (DTI),<sup>6</sup> which estimates the local WM orientation by using the property that water diffuses fastest parallel to the direction of the fiber bundles. WM pathways are estimated by WMT by using algorithms that detect long-range patterns of continuity in the diffusion tensor field.<sup>1-5</sup> Multiple studies have demonstrated that WMT can reconstruct the major WM fiber structures in healthy brain, with results that are in agreement with known anatomy derived from postmortem dissection studies.<sup>4</sup>

The unique capabilities of WMT for localizing, segmenting, and mapping WM structures make it a promising method for visualizing the relationship between WM and brain lesions. Such knowledge may be useful for presurgical assessments. Several recent studies have reported using maps of the DTI eigenvector<sup>7-12</sup> or WMT<sup>13-17</sup> for mapping the effects of neoplasia on WM anatomy. DTI and WMT may be used to assess whether tumors infiltrate, displace, or disrupt WM structures.<sup>8,10,11</sup>

Similarly, DTI and WMT may be used to evaluate the effect

of surgery on the WM anatomy. Resection of tissue may cause significant reorganization of brain structures, which may be monitored by using DTI.<sup>9,18</sup> Recently, a small preliminary study found that clinical motor performance correlated with the WM changes observed in the DTI data before and after tumor resection.<sup>19</sup> In most cases, the eigenvector color maps are adequate for visualizing the relationship between lesions and specific WM tracts. However, WMT is more useful in mapping complex WM pathways and potentially segmenting portions of WM structures.<sup>20,21</sup> Few studies to date have applied WMT to the evaluation of WM anatomy before and after tumor resection.<sup>22</sup> A recent study used WMT to evaluate tract shifts during surgery with respect to preoperative positions.<sup>23</sup>

The aim of this study was to investigate the potential role of WMT for mapping WM tracts in relation to cerebral mass lesions before and after surgical resection. Eigenvector color maps were used to initially assess the specific WM tracts that appeared to be either disrupted or displaced by the tumor. WM tractograms of affected WM structures were generated to evaluate the impact of the lesion initially and the surgery subsequently in 6 patients. Tracts were evaluated by using the degree of spatial symmetry with unaffected contralateral tracts and the continuity of the WMT connectivity patterns.

## Methods

### Patient Population

Six patients with either a brain neoplasm or a vascular malformation were included in this study, which was performed in compliance with the guidelines of the institutional review board. Patient age varied between 2 and 61 years (SD, 22 years). DTI data were obtained before and after surgical resection of the lesion. Postsurgical imaging was

Received April 20, 2005; accepted after revision October 31.

From the Laboratory for Brain Imaging and Behavior (M.L., P.J.T., A.L.A.), and the Departments of Biomedical Engineering (P.J.T.), Radiology (A.S.F.), Neurological Surgery (B.B.), Medical Physics (A.L.A.), and Psychiatry (A.L.A.), University of Wisconsin, Madison, Wis.

This work was supported in part by NIH grants R01 MH062015 and R01 EB002012.

Presented at the 12th annual meeting of the International Society for Magnetic Resonance in Medicine, Kyoto, Japan, May 15–22, 2004.

Address Correspondence to: Mariana Lazar, PhD, Laboratory for Brain Imaging and Behavior, The Waisman Center, 1500 Highland Ave, Madison, WI 53705.

performed between 1 week and 8 months (median, 6 months) after resection. The pathology included 3 astrocytomas, 1 ganglioglioma, and 2 cavernous angiomas.

### Clinical Evaluation

All patients included in this study underwent detailed neurologic examinations conducted by a physician blinded to the DTI findings. The neurologic evaluation was performed by the same physician for all patients, before and after the surgery. Motor strength in each patient was assessed for upper and lower extremities by using the Medical Research Council Scale of 0–5,<sup>24</sup> in which 5 indicates that muscle contraction overcame full resistance; 4, muscle contraction was reduced but able to overcome some resistance; 3, muscle contraction was able to overcome only gravity; 2, muscle contraction occurred only when the force of gravity was eliminated; 1, muscle produced only trace movement or fasciculation; and 0, no muscle contraction was observed. Scores that were reported between scale levels (eg, 3+ or 4–) were taken as the lower value (ie, 3+ / 4– = 3). Motor findings were obtained from inpatient charts or outpatient clinic notes. Clinical assessment of patients 2, 3, and 6 was first presented in a previous study.<sup>19</sup> The remaining patients (1, 4, and 5) were excluded from that study due to potential involvement of the motor cortex.

### Diffusion Tensor Imaging

Diffusion tensor imaging was performed on a 1.5T Signa scanner (GE Healthcare, Waukesha, Wis) with CV/i gradients (40 mT/m maximal amplitude; 150 mT/m per millisecond slew rate) by using the product quadrature birdcage head coil. A single-shot spin-echo echo-planar imaging pulse sequence with diffusion-weighting gradients was used to obtain DTI images. Twenty-three encoding directions (with constant diffusion-weighting,  $b = 1000$  seconds/mm<sup>2</sup>) were used for diffusion tensor encoding. Other imaging parameters were the following: TR/TE, 4500/71.8 ms; number of excitations, 4 (magnitude image averaging); field of view, 240 mm; data acquisition matrix, 128 × 128; and section thickness, 3 mm with a 0-mm gap. Images were zero-fill interpolated during reconstruction to a 256 × 256 image matrix. Between 21 (1 slab) and 42 (2 slabs) axial sections were acquired to cover the brain region affected by the lesion. The full cerebrum was covered with the 42-section protocol. The total image acquisition time varied between 7 and a half and 15 minutes, depending on the number of sections acquired.

### Diffusion Tensor Processing

Misregistration of diffusion-weighted images related to patient motion and eddy current distortions was corrected by using an affine 2D linear registration algorithm in automated image registration.<sup>25</sup> When 2 slabs were acquired, the data were merged into a single volume by using an overlapping section for registration. The imaged volume was then interpolated for all the datasets to isotropic voxel

dimensions of 0.9375 mm. The diffusion tensor elements, as well as the trace, eigenvalues, eigenvectors, and several anisotropy measures (including the fractional anisotropy [FA] and linear and planar metrics) were calculated at each voxel of the image volume. The major eigenvector components of the tensor,  $e_x$ ,  $e_y$ , and  $e_z$ , (weighted by FA) were mapped into RGB (red, green, blue) color space to generate color maps.<sup>26</sup> This mapping represents the tracts oriented from right to left in red, tracts oriented anteroposteriorly in green, and tracts oriented inferosuperiorly in blue (with all other orientations represented by a mixture of these colors).

### White Matter Tractography

Fiber tracking was performed by using the tensor deflection algorithm.<sup>5</sup> First, fiber trajectories were generated from regions enclosing a cross-section of the tracts of interest. The propagation of an individual trajectory was generally terminated when it reached a voxel with FA < 0.2 or when the angle between 2 consecutive steps was >45°. In cases in which tracts entered regions of abnormally low anisotropy, resulting in potentially premature termination, the FA threshold was lowered while maintaining the angle threshold. This relaxation of the anisotropy threshold was performed to determine whether continuous coherent (see “Image Interpretation” for a definition) trajectories could be obtained in these regions. The choice of threshold in these cases was based on the local tract anisotropy. Note that by maintaining the angle threshold while relaxing the anisotropy threshold, we found that the stopping criteria were “reasonable,” (ie, they impeded the generation of recognizably spurious tracts but did not penalize tract-mapping for low anisotropy). The FA threshold was reported in each case in which it differed from the default value of 0.2. After the original set of trajectories was generated, a multiple region-of-interest approach<sup>4</sup> was used to select the tracts of interest. Unlikely trajectories were removed from the original set.

### Image Interpretation

Fiber trajectories were considered connected to a certain region (eg, motor cortex) if one of their ends terminated into that region; trajectories were considered to represent connectivity patterns between the 2 regions into which their ends terminated. Trajectories of a tract were considered to be “interrupted” (as opposed to “continuous”) if they failed to connect regions that are known to be anatomically connected (eg, trajectories of the inferior fronto-occipital fasciculus that originate near the occipital cortex and appear to follow the known tract course but terminate before reaching the frontal cortex). Trajectories of a set were considered “coherent” if their paths ran relatively parallel to each other in the trunk region of a structure and diverged/converged in an ordered fashion as the structure fanned or merged near cortical regions. “Coherence,” as defined here, was considered to be indicative of at least partial preservation of tract structure in cases in which tracts were characterized regionally by abnormally low anisotropy.

**Table 1: Clinical assessment of motor function before and after surgery**

Patient No.	Preoperative Assessment	Postoperative Assessment	Notes
1	4/5 right upper/lower extremity	Normal	Potential involvement of motor cortex
2	4/5 right upper/lower extremity	Normal	—*
3	3–4/5 right upper/lower extremity	Normal	—*
4	4/5 left upper/lower extremity	Normal	Potential involvement of motor cortex
5	Normal	Normal	Potential involvement of motor cortex
6	Normal	Normal	—*

\*Clinical assessment of patients 2, 3, and 6 was first presented in Laundre et al.<sup>19</sup>

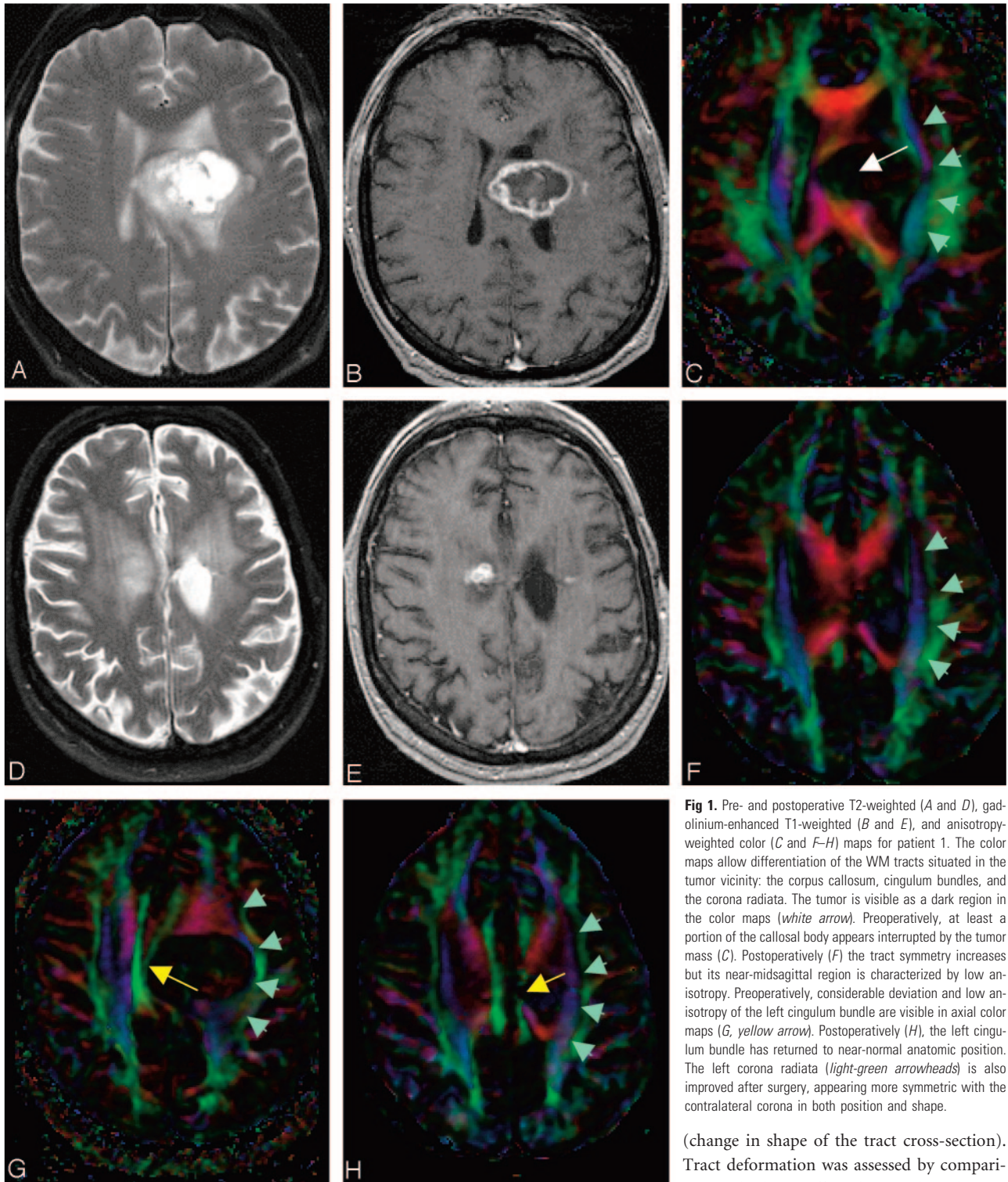


**Fig 1.** Pre- and postoperative T2-weighted (*A* and *D*), gadolinium-enhanced T1-weighted (*B* and *E*), and anisotropy-weighted color (*C* and *F-H*) maps for patient 1. The color maps allow differentiation of the WM tracts situated in the tumor vicinity: the corpus callosum, cingulum bundles, and the corona radiata. The tumor is visible as a dark region in the color maps (*white arrow*). Preoperatively, at least a portion of the callosal body appears interrupted by the tumor mass (*C*). Postoperatively (*F*) the tract symmetry increases but its near-midsagittal region is characterized by low anisotropy. Preoperatively, considerable deviation and low anisotropy of the left cingulum bundle are visible in axial color maps (*G*, *yellow arrow*). Postoperatively (*H*), the left cingulum bundle has returned to near-normal anatomic position. The left corona radiata (*light-green arrowheads*) is also improved after surgery, appearing more symmetric with the contralateral corona in both position and shape.

ropy values. Abnormal anisotropy of a tract region was defined by comparison with the normal contralateral WM region.

Several patterns of tract alteration were identified and classified as follows: A tract was considered “deviated” if it was characterized by abnormal location and/or direction as a result of the lesion mass effect. Incorrect location was assessed by comparison with the homologous tract situated in the contralateral hemisphere or, when this characterization was not possible (eg, the corpus callosum), by comparison with known normal anatomy. In cases with substantial mass effect, tract deviation was sometimes associated with “deformation”

(change in shape of the tract cross-section). Tract deformation was assessed by comparison with the unaffected contralateral tract.

Tract deviation sometimes occurred in a “splayed” pattern (ie, when the lesion appeared to separate a tract into distinct bundles deviated in different directions). A tract was considered “interrupted” if any portion of the tract was visibly discontinuous on anisotropy-weighted directional color maps and fiber-tracking terminated at the discontinuity despite reasonable relaxation of stopping criteria (“reasonable” as defined previously). Note that a tract may be interrupted either partially or completely. A tract was considered “infiltrated” if any portion of it showed significantly reduced anisotropy while retaining sufficiently ordered structure to allow its identification on directional

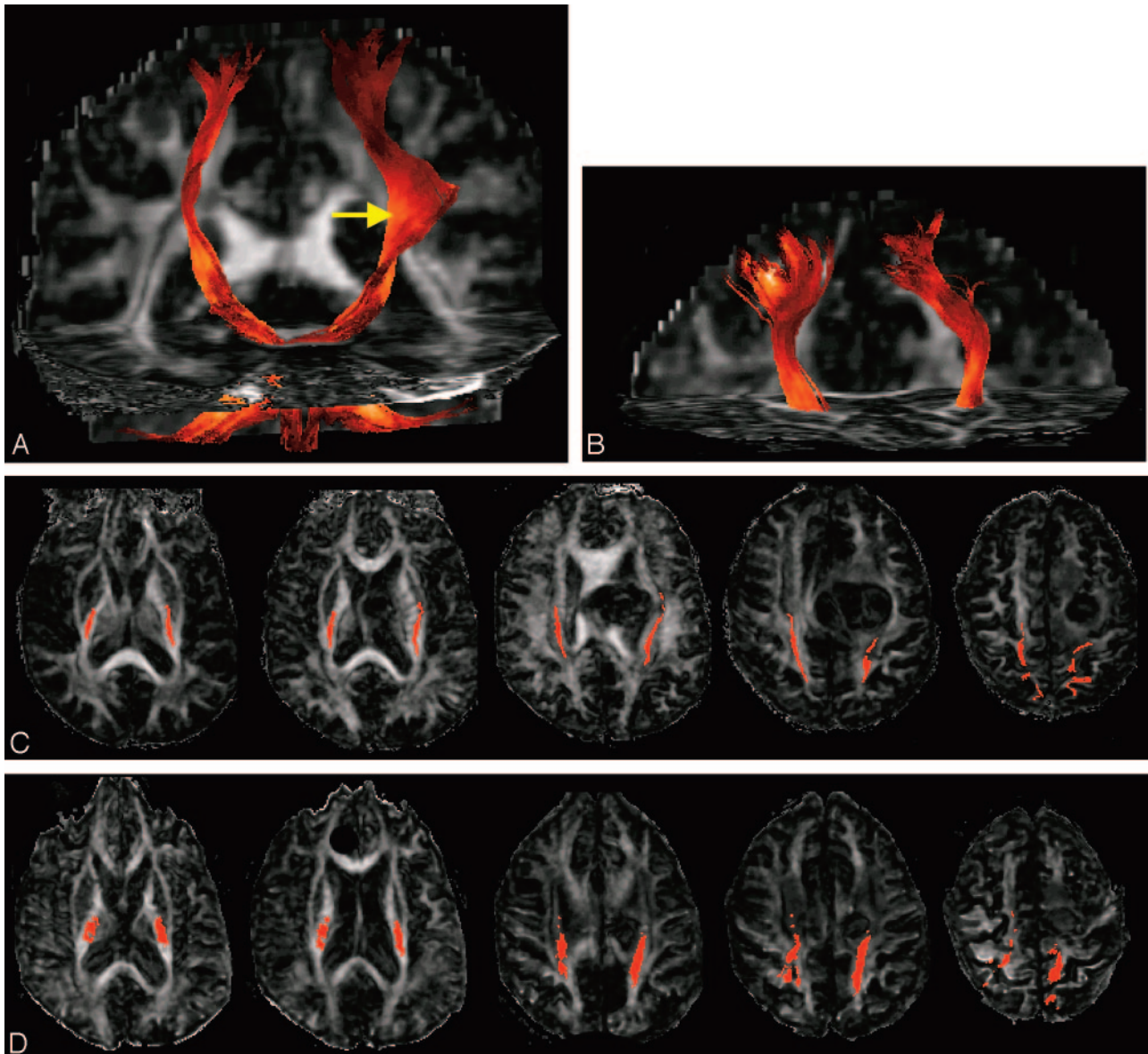


**Fig 2.** Tractograms of the cortico-spinal tracts before (A) and after (B) surgery for patient 1. The color of the fiber trajectories relates to local anisotropy, with yellow indicating high anisotropy and dark red, low anisotropy. The corresponding tract positions are shown superimposed onto axial FA maps in (C) and (D), respectively. Deviation and deformation of the ipsilateral tract in the tumor proximity are apparent in the preoperative tractogram (yellow arrow).

color maps and to allow fiber-tracking to proceed. Note that infiltration by tumor is not discriminated from infiltration by edema because this problem has yet to be solved.<sup>10,11</sup> A tract was considered “degenerated” if it was characterized by significantly reduced size and/or anisotropy at a substantial distance from a lesion affecting the same neural pathway (either cortical or subcortical), such that secondary wallerian degeneration, rather than infiltration, could reasonably be presumed (eg, a chronically atrophic-appearing pyramidal tract in the brain stem, distal to a noninfiltrating lesion of the corona radiata).

Note that these patterns are not mutually exclusive: Tract deviation might be accompanied by partial tract infiltration or interruption. Tract characterization in each case was confirmed by a board-certified neuroradiologist familiar with tract anatomy (A.S.F.).

## Results

The results of the clinical evaluation for all patients are shown in Table 1. Four patients who presented with reduced motor

function before surgery showed a return to normal function following surgery. Two patients who presented with normal motor performance before surgery maintained their level of performance after surgery.

Patient 1 presented with a grade III astrocytoma situated in the superior medial region of the left frontal lobe (Fig 1). The tumor interrupted the central portion of the corpus callosum and deviated the left cingulum bundle medially. The ipsilateral cingulum bundle appeared to be characterized by lower FA than the contralateral bundle in the tumor vicinity (region of interest mean  $\pm$  SD,  $0.28 \pm 0.08$  compared with  $0.48 \pm 0.18$  for the contralateral bundle). The ipsilateral corona radiata was deviated laterally, with tract deviation and deformation visible in axial and coronal color maps. A follow-up DTI was performed 8 months after surgical resection. The appearance of the corpus callosum improved, as shown by higher inter-hemispheric tract symmetry (Fig 1F). However, the tract ap-

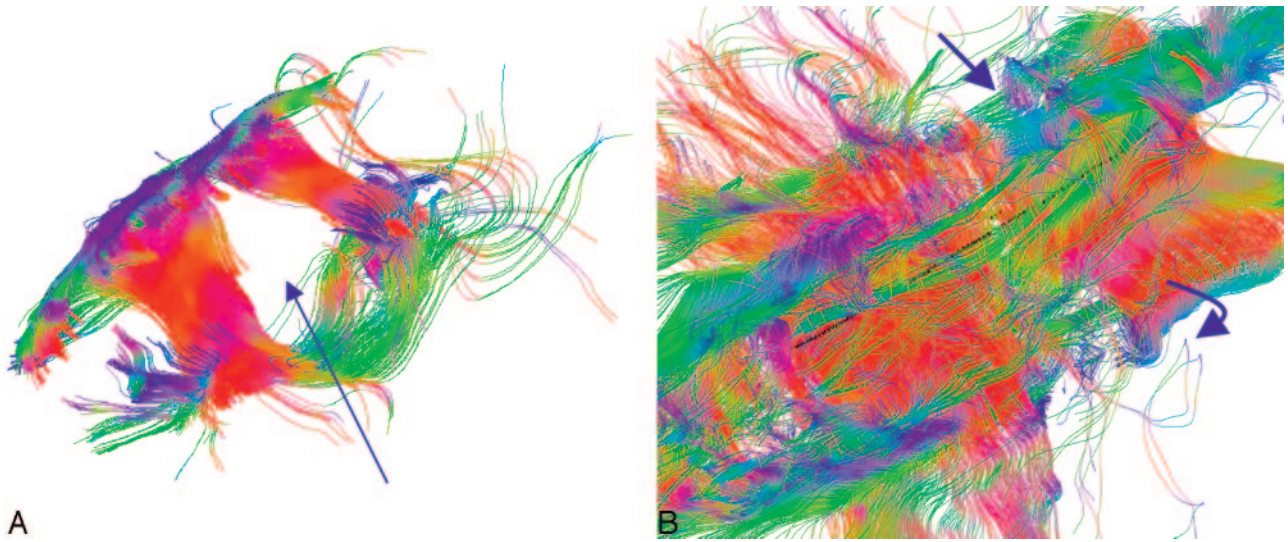


**Fig 3.** Tractograms of the corpus callosum before (A) and after (B) surgery for patient 1. The color of the trajectories indicates the local tract orientation by using the RGB convention. Preoperatively, many trajectories of the callosal body appear deviated and several appear interrupted by the tumor mass (*arrow*). Postoperatively, coherent trajectories appear to cross the midline; however, abnormal trajectories also appear to be present (*blue arrows*). The position of the seed points in both tractograms is indicated by black dots. The postoperative tractogram of the corpus callosum was generated by using a FA threshold of 0.04.

peared thinner in the sagittal section and was characterized in the midsagittal body region by low FA ( $0.23 \pm 0.09$  compared with  $0.72 \pm 0.06$  for the splenium region). The ipsilateral cingulum bundle returned closer to the normal anatomic position, running parallel to the less-affected contralateral bundle

(Fig 1H). The left corona radiata also appeared to return to a more normal position as depicted by the higher degree of symmetry between the left and right hemispheres.

WMT was used to reconstruct the corpus callosum, the cingulum bundles, and the corticospinal tracts. Tractograms

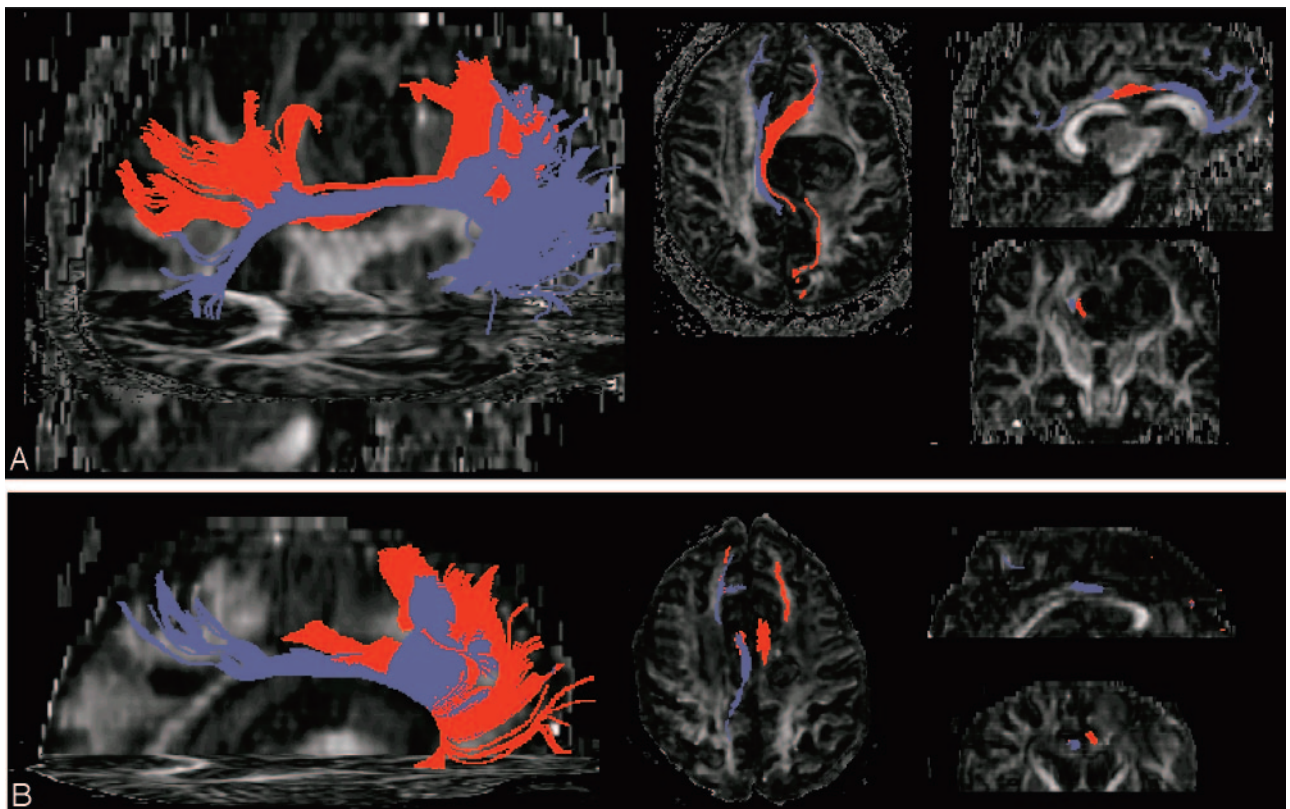


**Fig 4.** Pre- (A) and postoperative (B) tractograms of the cingulum bundles for patient 1. The tractograms were generated from a set of seeds placed in the anterior region of the tract. The relative positions of the ipsilateral (red) and contralateral (purple) bundles are labeled onto axial, sagittal, and coronal FA maps. Postoperatively, the ipsilateral bundle terminates before reaching the posterior region of the tract.

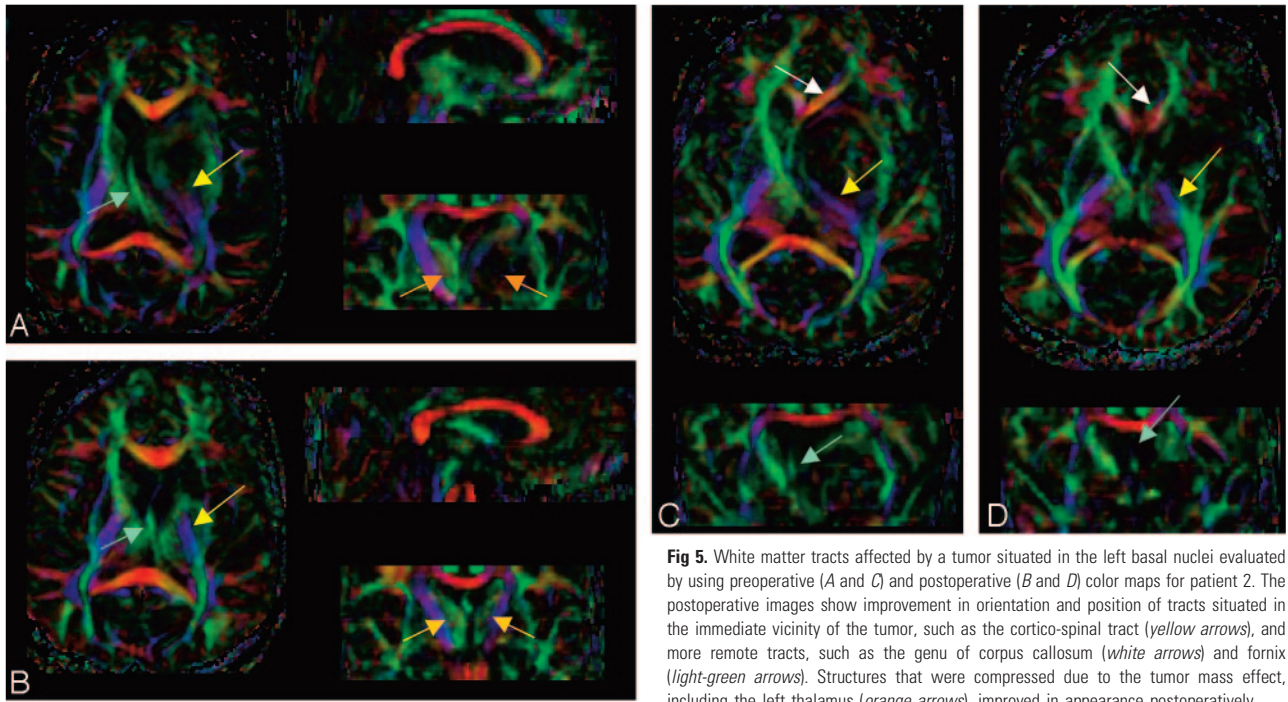


**Fig 5.** White matter tracts affected by a tumor situated in the left basal nuclei evaluated by using preoperative (*A* and *C*) and postoperative (*B* and *D*) color maps for patient 2. The postoperative images show improvement in orientation and position of tracts situated in the immediate vicinity of the tumor, such as the cortico-spinal tract (*yellow arrows*), and more remote tracts, such as the genu of corpus callosum (*white arrows*) and fornix (*light-green arrows*). Structures that were compressed due to the tumor mass effect, including the left thalamus (*orange arrows*), improved in appearance postoperatively.

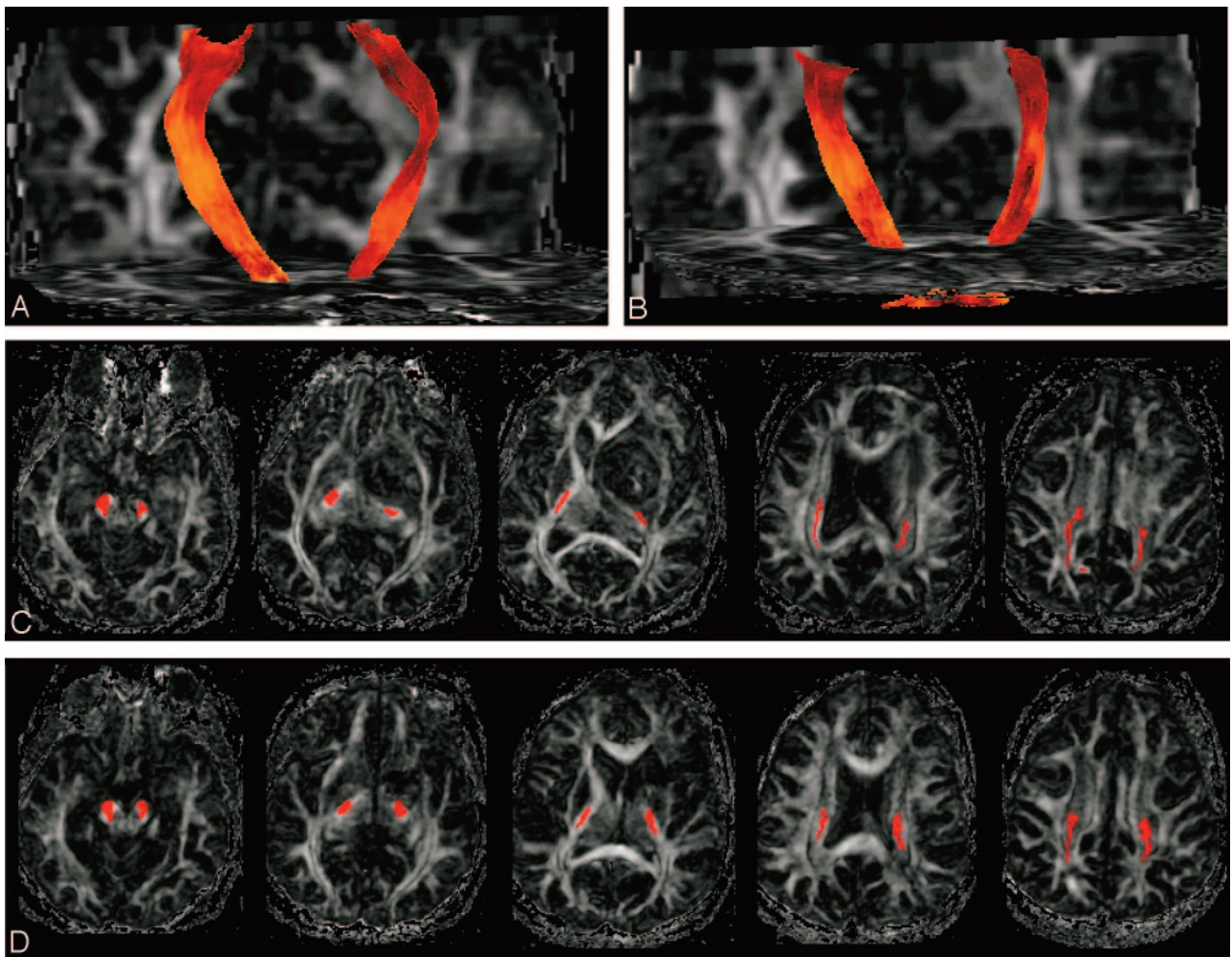


**Fig 6.** Tractograms of the corticospinal tracts superimposed onto preoperative (*A* and *C*) and postoperative (*B* and *D*) axial FA maps for patient 2. *C* and *D*, Similar axial sections were used to indicate the anatomic locations of the tracts. Coherent and uninterrupted pathways were obtained for both pre- and postoperative tractograms. Postoperatively, the ipsilateral corticospinal tract returns to near-normal anatomic position and becomes more symmetric with respect to the contralateral tract.

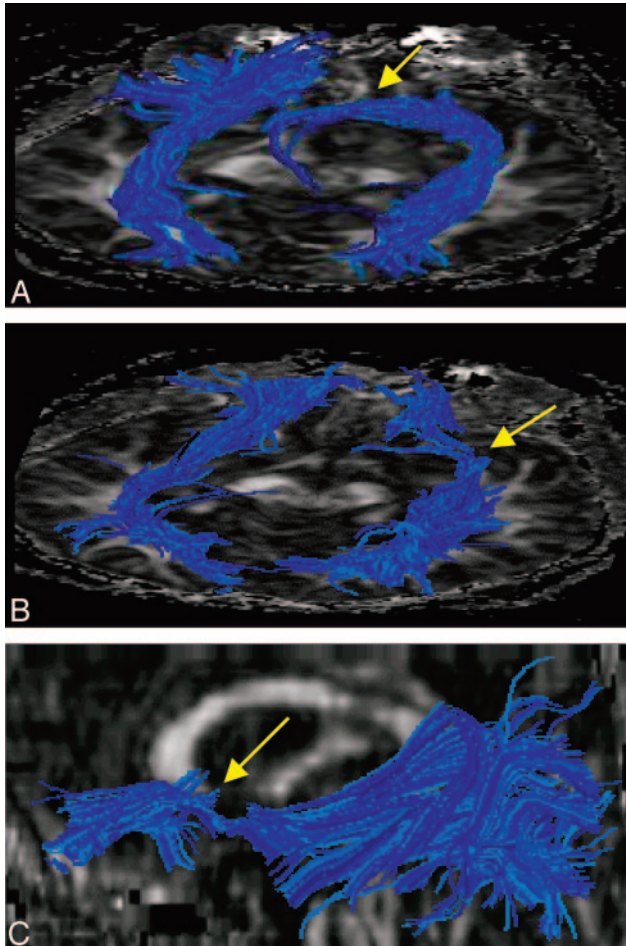


**Fig 7.** Pre- (*A*) and postoperative (*B* and *C*) tractograms of the inferior fronto-occipital fasciculi in patient 2. *B* and *C*, Two different views of the postoperative tract reconstruction. The tract appears altered before and after surgery. A set of anomalous trajectories that course toward midline before reaching the frontal cortex is observed preoperatively in the anterior portion of the tract (*A*, yellow arrow). Postoperatively (*B* and *C*), most of trajectories originating in either the frontal or temporal lobes appear to terminate near the resection site (yellow arrows).

of the corticospinal tracts (Fig 2) show that preoperatively the ipsilateral tract appeared deviated and deformed because of the tumor mass effect. The tract returned to a normal anatomic position after the surgery (Fig 2*B*, -*D*). This normalization in tract position was accompanied by improvement in motor function (Table 1). The preoperative corpus callosum trajectories were interrupted and deviated by the tumor (Fig 3*A*). After surgery, continuous trajectories across the brain midline were observed when the FA threshold was reduced to 0.04 (Fig 3*B*). Note that whereas coherent trajectories appear to cross the midline, abnormal pathways are also present. This may be caused by partial volume averaging and an increased uncertainty in tract direction in the low anisotropy regions. The reduction in FA threshold used for tract termination did not result in an increased number of interhemispheric trajectories in the preoperative corpus callosum.

The preoperative cingulum bundle tractograms (Fig 4*A*) showed deviated but coherent ipsilateral tract estimates. Post-resection, the ipsilateral bundle returned to a more normal anatomic position as indicated by the color images in Fig 1,

though the tract reconstructions were unable to continuously trace the cingulum bundle (Fig 4*B*). Fiber-tracking initiated from both the anterior and posterior cingulum regions of interest showed that the trajectories terminated in the vicinity of the resection site (not shown).

Patient 2 presented with a pilocytic astrocytoma centered in the left basal nuclei, displacing the corticospinal tracts, external capsule, fornix, and genu of the corpus callosum (Fig 5). The structural displacements caused by the mass effect were significantly reduced 6 months after resection as depicted in Fig 5*B*, -*D*. WMT reconstructions of the corticospinal tracts demonstrated that the left tract was deviated posteriorly but returned intact to roughly the normal anatomic position after surgery (Fig 6). The normalization in tract position was accompanied by improvement in the motor function of the patient (Table 1). The inferior fronto-occipital fasciculi were also reconstructed as shown in Fig 7. Before surgery, the ipsilateral fiber trajectories, which should project to the frontal lobe, demonstrated aberrant connection patterns, with some trajectories originating in the occipital lobe, either terminating or apparently veering toward brain midline (arrow) before reaching the frontal lobe. Figures 7*B* and *C* display 2 different views of the postoperative tractogram. After surgery, the tract patterns appeared more anatomic, though the region near the site of resection demonstrated considerable thinning with partial tract interruption. Some of the trajectories originating in either the occipital or frontal lobe terminated near the resection site. Lowering the anisotropy threshold did not result in a substantially increased number of continuous trajectories connecting the occipital and frontal lobes.

Patient 3 presented with a ganglioglioma involving the left cerebral peduncle and deviating in a splaying fashion the fibers of the right corticospinal tract anteromedially and posterolaterally. Figure 8 shows the corticospinal tract trajectories before and 5 months after surgery. WMT shows coherent fiber trajectories for the main bundle and the bundles that have been splayed by the lesion. On the basis of the appearance of tract volume at the cerebral peduncle level and in comparison with the contralateral hemisphere, the bulk of the tract appears to be contained in separated bundles. The trajectories appear to course around the tumor and do not terminate in the tumor vicinity. However, even if not detectable by WMT, some minor tract interruption might be present. The tract appeared closer to the normal anatomic position after surgery. This improvement in corticospinal tract appearance was accompanied by a return of normal motor function (Table 1).

Patient 4 presented with a grade IV astrocytoma centered in the right centrum semiovale. The tumor deviated the superior longitudinal fasciculus, corona radiata, corpus callosum, and right cingulum bundle. WMT reconstruction of the projection fibers of the internal capsule and corona radiata (including the corticospinal tract, Fig 9) preoperatively demonstrated that the WM bundles maintained coherence even through regions of low anisotropy. The low anisotropy associated with coherent trajectories suggested the presence of tract infiltration. Some deviation of the motor and sensory fibers (orange and green) was also apparent. Six months after surgery, the pattern of corona radiata bundles appeared more symmetric between hemispheres. The improvement in corticospinal tract appearance was accompanied by a return of nor-

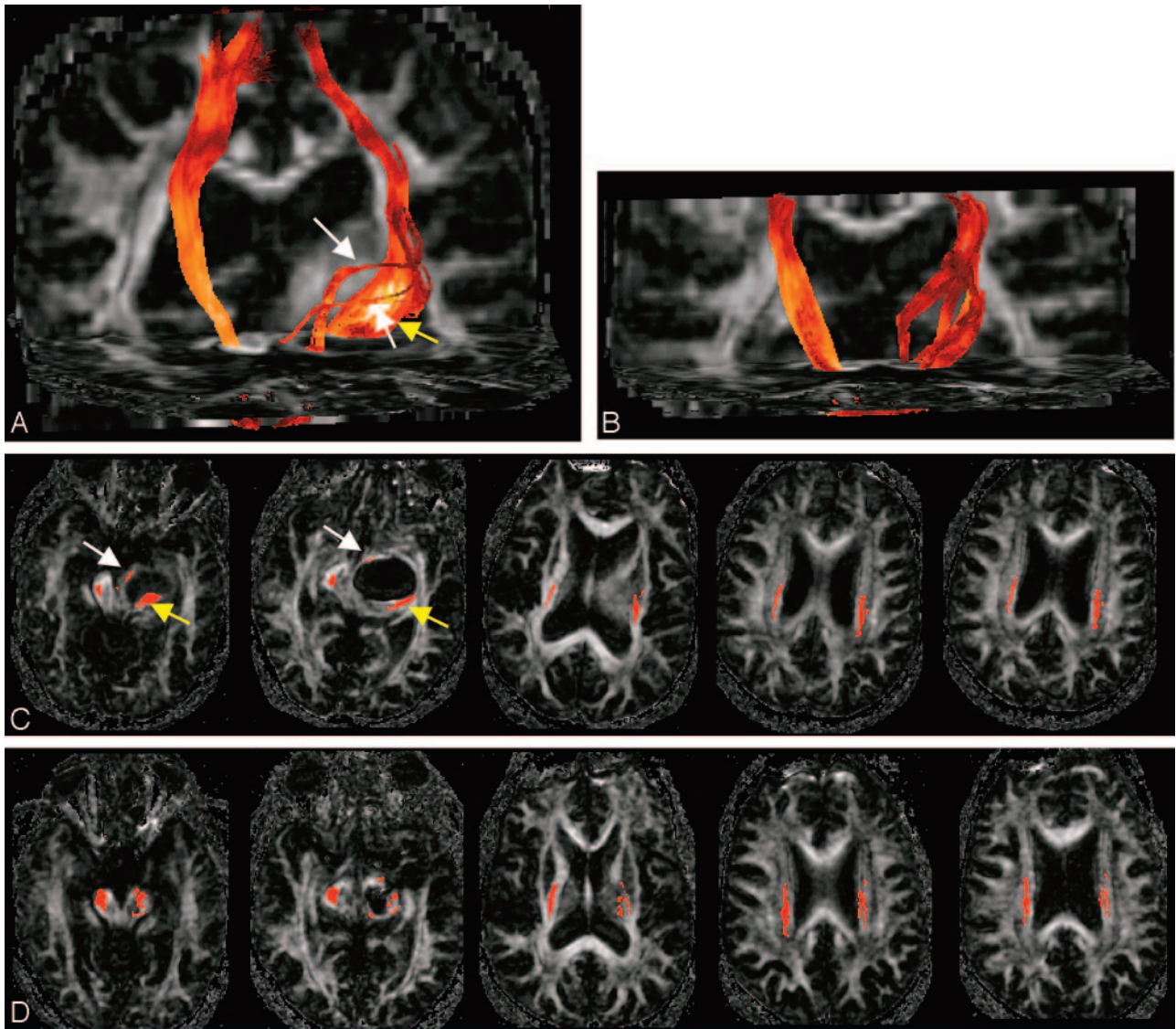


**Fig 8.** Tractograms of the corticospinal tracts superimposed on preoperative (A and C) and postoperative (B and D) FA maps for patient 3. C and D, Similar axial sections were selected to indicate the anatomic locations of the tracts. Preoperatively, trajectories originating from the cerebral peduncle and reaching the motor cortex in the ipsilateral hemisphere form 1 main bundle deviated posterolaterally (yellow arrow) and several thinner bundles deviated anteromedially (white arrow). These bundles appear stretched in the tumor vicinity. The ipsilateral tract appears preserved after the surgery and positioned closer to normal anatomic position, except in the immediate vicinity of the resection.

mal motor function (Table 1). The corpus callosum tractogram showed deviation and tract infiltration (suggested by low anisotropy with coherent trajectories) in the tumor vicinity preoperatively (images not shown). The tract appeared to return to a more normal position postoperatively, and the region of low anisotropy appeared reduced in size. A threshold of 0.04 was used to generate corpus callosum trajectories. Figure 10 shows the tractograms of the right superior longitudinal fasciculus before and after surgery. Coronal cross-sections depict the positions of both superior longitudinal fasciculi; the position of the right superior longitudinal fasciculus returned to a more normal anatomic position after tumor resection.

Patient 5 presented with a giant cavernous angioma displacing the left corona radiata medially (Fig 11). Color maps and tractograms show improvement in the ipsilateral tract position after surgery. The preoperative tractogram shows corti-

cospinal tract trajectories connecting the motor cortex with the brain stem (Fig 12A), but deviating medially. The postsurgical tractogram (Fig 12B) indicates both tract preservation and a return to the normal anatomic organization. Corticospinal tract preservation was accompanied by preservation of normal motor function in this patient.

Patient 6 presented with a cavernous angioma centered in the right striatal region and slightly deviating the corticospinal tracts (Fig 13). Tractograms also indicated that corticospinal tract connectivity was not affected by the cavernoma and remained preserved after surgery (Fig 14). This near-normal appearance of the corticospinal tracts was accompanied by normal motor function preoperatively and preservation of normal motor function postoperatively. Preoperative and postoperative (8 months) tractograms (Fig 15) depicted the preservation of ipsilateral inferior fronto-occipital and uncinate fasciculi. Before surgery, the ipsilateral tracts appeared

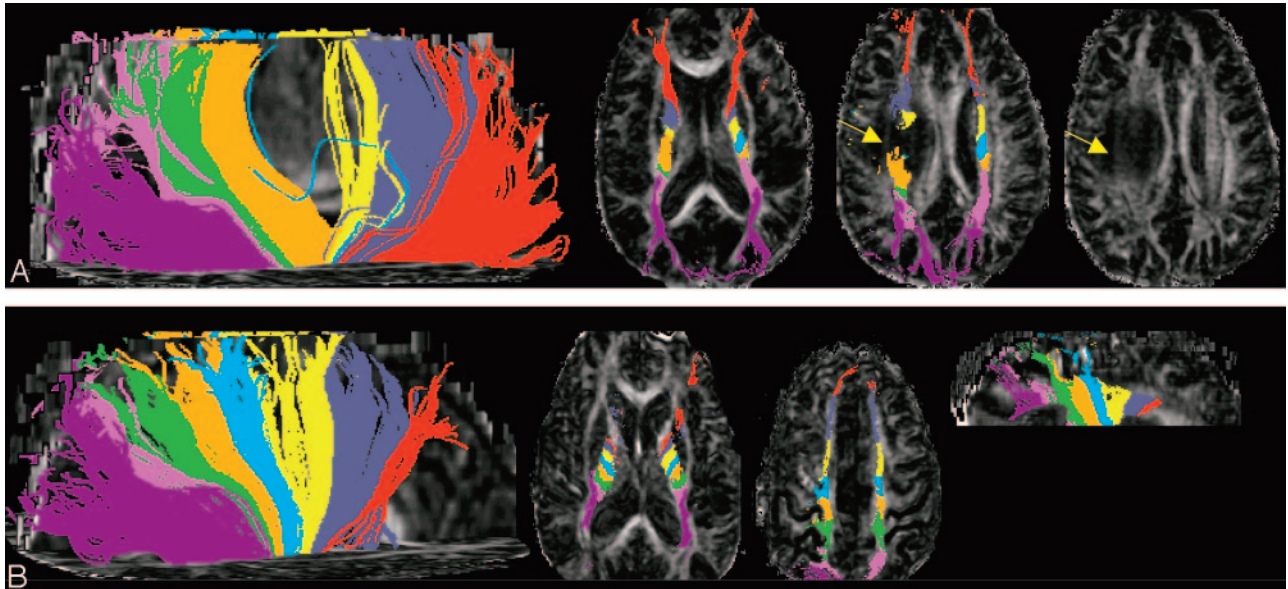


**Fig 9.** Tractograms of the projection fibers and corona radiata pre- (*A*) and postoperatively (*B*) for patient 4. An FA threshold of 0.08 was used for terminating fiber trajectories. The trajectories are color-coded according to their anteroposterior position. Their relative position is shown in axial and sagittal FA maps. Continuous trajectories were obtained even through regions of low anisotropy (*arrows, A*).

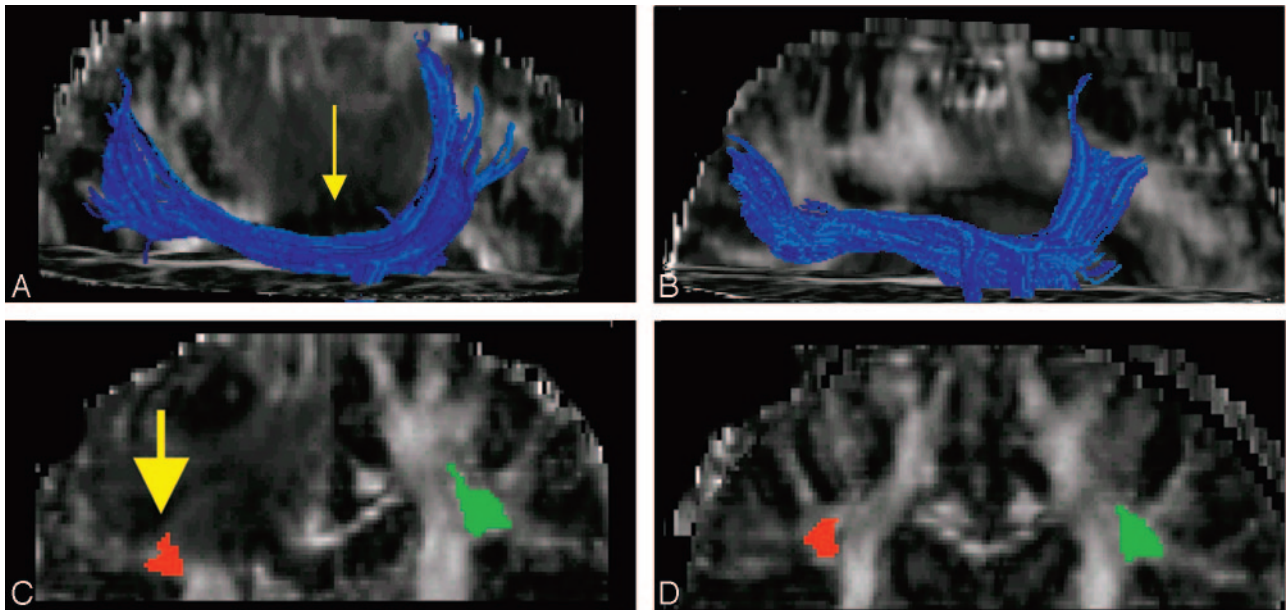


**Fig 10.** Pre- (*A*) and postoperative (*B*) tractograms of the ipsilateral superior longitudinal fasciculus for patient 4. The relative anatomic positions of the ipsilateral (red) and contralateral (green) tracts are shown superimposed onto coronal FA maps for the pre- (*C*) and postoperative (*D*) images. Preoperatively, the tract is deviated inferiorly because of the mass effect of the tumor (*arrows*) and consequently is positioned lower than the contralateral tract in coronal cross-section. Postoperatively, the tract appears to return to a more normal anatomic position and is positioned symmetrically with respect to the contralateral tract.

slightly deviated inferiorly, but they returned to a more symmetric position after surgery.

The WMT findings for the 6 patients are summarized in Table 2.

### Discussion

In this study, DTI and WMT were used to characterize non-invasively the effects of space-occupying lesions and their resection on WM structures in a small number of patients. In general, these cases demonstrated that DTI and WMT are useful for preoperative planning and for monitoring the structural remodeling of the brain after surgery. In all patients after

resection, the WM organization appeared more symmetric and anatomic when deviated tracts were preserved.

In most cases, the principal eigenvector color maps were useful for identifying specific WM tracts and mapping the relationship between the WM and either the lesion or the area of resection. However, in some cases, WMT was better able to map the complex spatial relationships between WM tracts and lesions in 3D. For example, WMT revealed the splaying of the corticospinal tracts around the tumor in patient 3 (Fig 8) and the apparent corticospinal tract deviation with deformation in patient 1 (Fig 2).

In every case described here, the postoperative WM tracto-

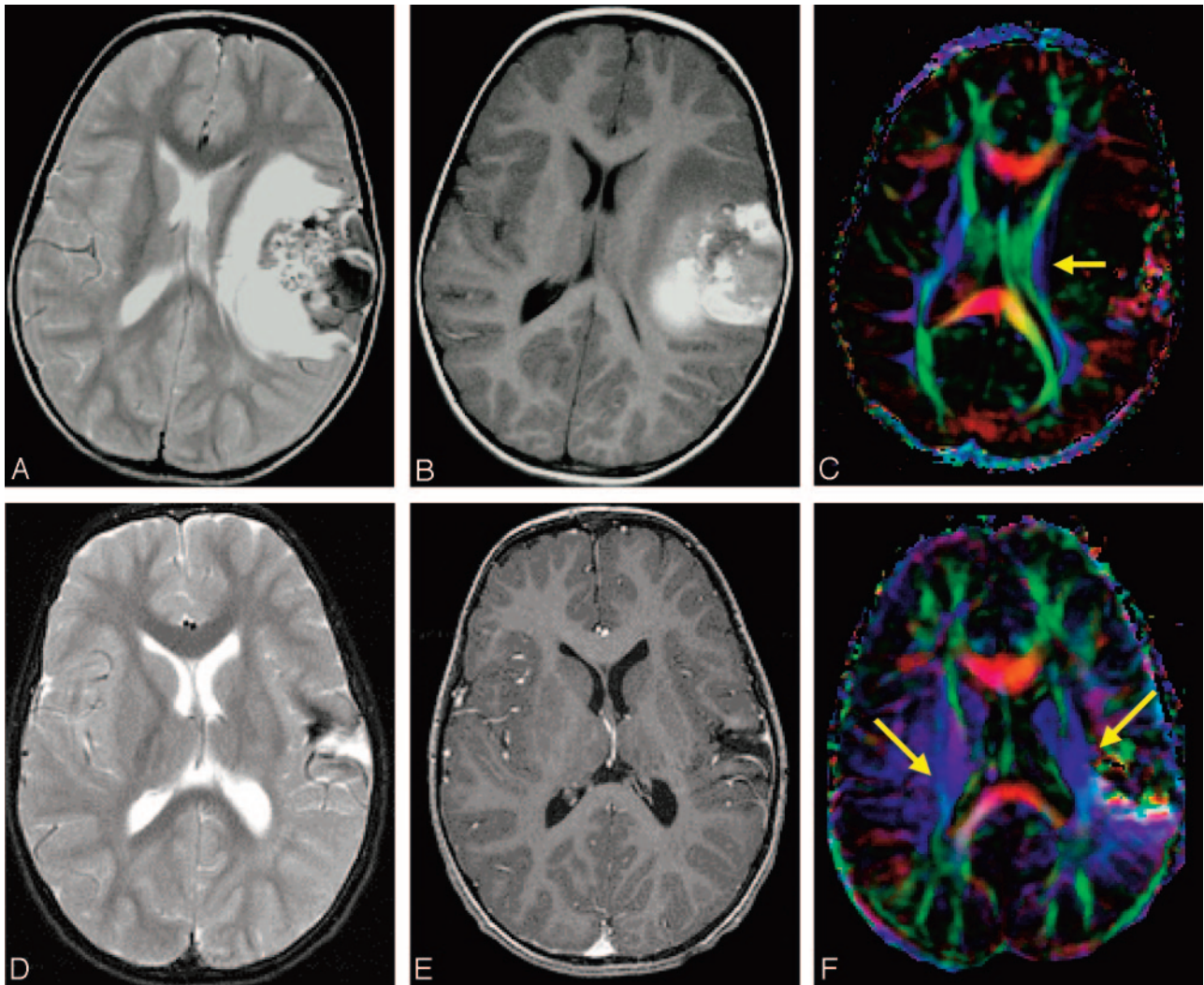


**Fig 11.** Pre- (A–C) and postoperative (D–F) axial images for patient 5: T2-weighted images (A and D), T1-weighted images (B and E), and directional color maps (C and F). Before surgery, the color images show posteromedial deviation and deformation (compression) of the posterior limb of the internal capsule (arrow, C). After surgery, the tract appears more symmetric with the contralateral tract (arrows, F) in position, cross-sectional shape, and orientation.

grams showed that the corticospinal tract was preserved during surgery and returned to a more normal position and organization. For all patients presented here, these results correlated before and after surgery with clinical evaluations that showed the same level or improvement of motor function. In 3 patients (1, 4, and 5), the lesion affected the motor cortex, potentially confounding the relationship between tract involvement and motor function. In the remaining 3 patients (2, 3, and 6), the lesions did not involve the motor cortex; therefore, motor function was presumably related to tract integrity. A previous study including patients 2, 3, and 6 similarly showed that preservation or improvement of motor function accompanied preservation or improved appearance of the corticospinal tracts on DTI color maps without tractograms.<sup>19</sup>

WMT is highly sensitive to noise<sup>27,28</sup> and image artifacts. A small perturbation in tract direction may cause tract estimates to jump to an incorrect pathway and lead to significant tract divergence. Thus, a certain degree of caution should be applied in the interpretation of any WMT result. This is partic-

ularly challenging in the presence of brain pathology, which may cause the tracts to deviate significantly from expected patterns. For example, in several cases presented here, the tract estimates appeared to terminate in the middle of a pathway (eg, the cingulum bundle in Fig 4B), to “jump” from 1 pathway to another (eg, the corpus callosum running into the association tracts in Fig 3A), or to follow an unlikely pathway (eg, anomalous right prefrontal projections of the inferior fronto-occipital fasciculi in Fig 7). These anomalies may be caused by one of several sources: (1) significant and real tract alteration (eg, actual tract injury from the lesion or surgery or acute tract deviations caused by the lesion), (2) errors in the tensor field from image noise or artifacts, or (3) partial volume averaging between intersecting and neighboring WM pathways.

In particular, the mass effect of the lesions and loss of tissue from surgical debulking may cause the tracts to be relatively thin, which will increase partial volume averaging effects.<sup>29</sup> Even in unaffected brain tissue, partial volume averaging can be significant and can make it impossible to resolve crossing WM pathways by using the simple diffusion tensor model.<sup>29</sup>

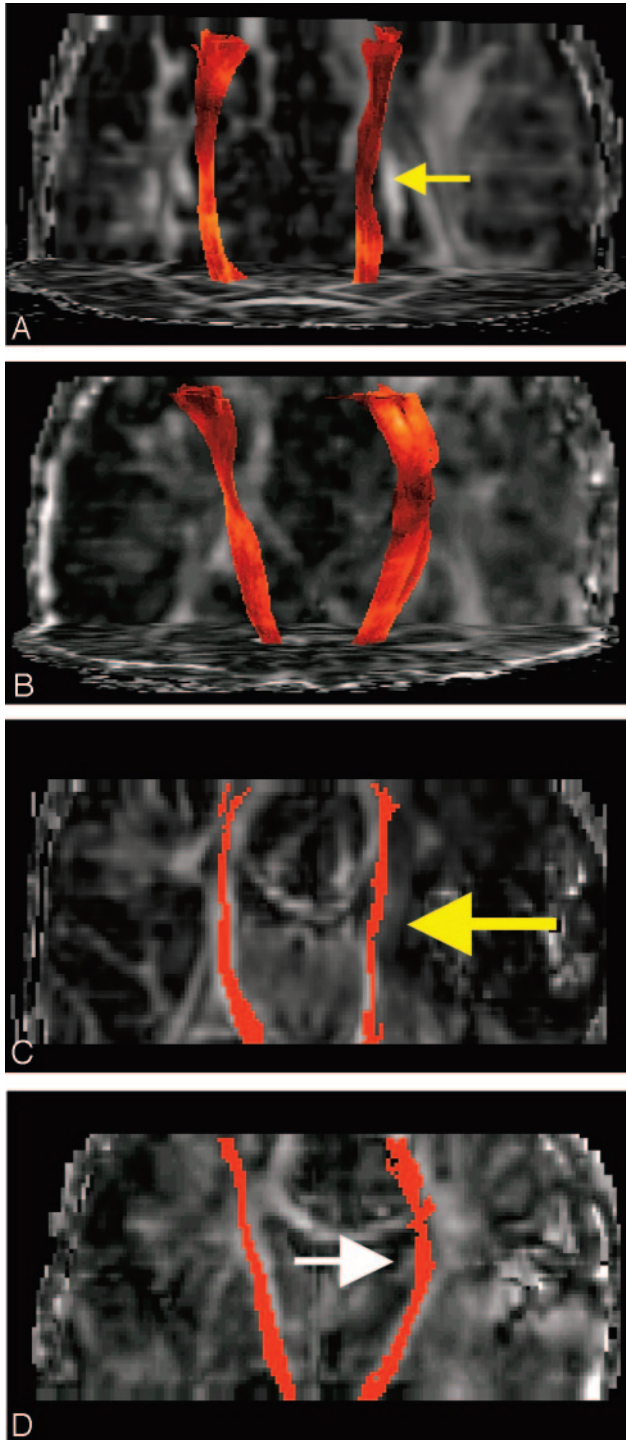


**Fig 12.** Pre- (A) and postoperative (B) tractograms of the ipsilateral and contralateral corticospinal tracts for patient 5. C and D, The corresponding tract positions in the coronal plane are shown before and after surgery, respectively. Preoperatively, the ipsilateral tract appears to be deviated medially due to the mass effect of the tumor (yellow arrows). Postoperatively, the tract returns to a more normal anatomic position (white arrow). An FA threshold of 0.15 was used to terminate trajectories for both pre- and postoperative tractograms.

Recently, more complex diffusion models and acquisition methods have been developed that are promising for resolving the organization of crossing WM.<sup>30,31</sup> Future developments to diffusion MR imaging methods and fiber tracking algorithms will likely improve the accuracy of WMT.

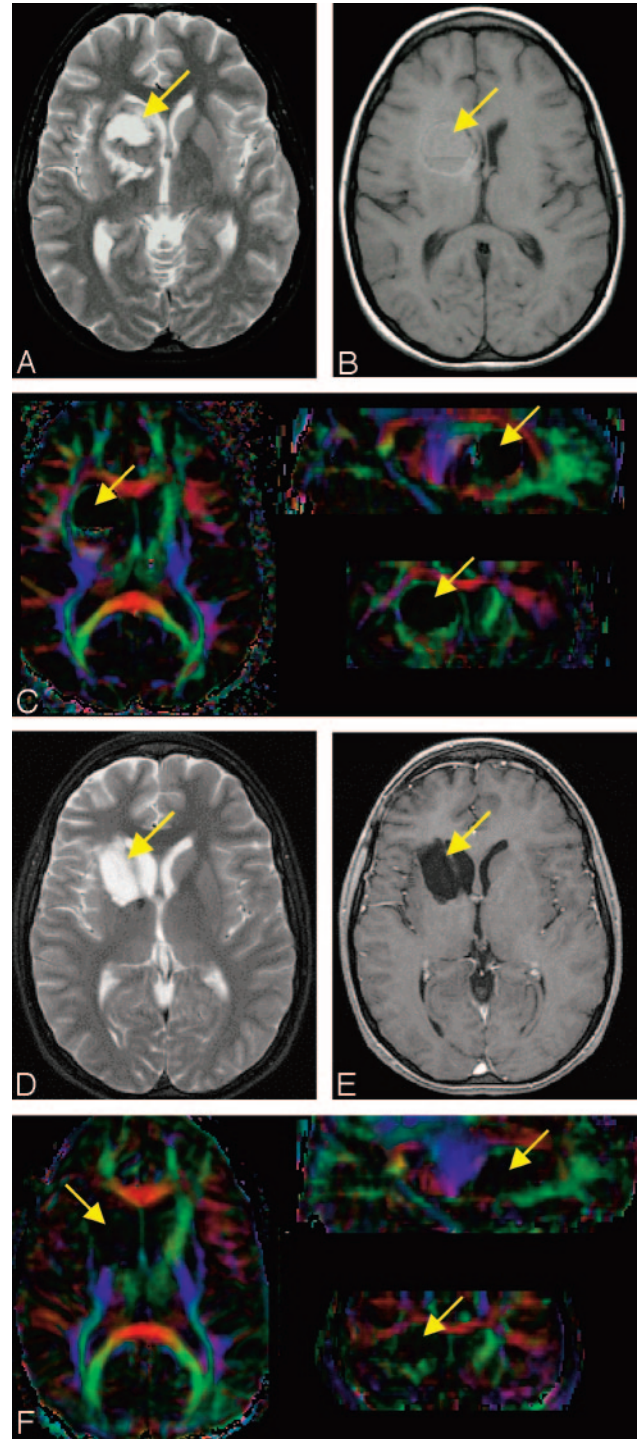


**Fig 13.** Cavernoma (A–C) and resection site (D–F) positions indicated by arrows in axial T2- (A and D) and T1-weighted (B and E) images and 3-plane cross-sectional color maps (C and F) for patient 6. C, The cavernoma appears to deviate the right corticospinal tracts posteriorly and the fornix medially. The lesion appears to interrupt the anterior limb of the internal capsule and deform (compress) the external capsule and inferior fronto-occipital fasciculus. Postoperatively (F), the fornix and the corticospinal tracts return to normal anatomic positions.

The current technical limitations of WMT and DTI, coupled with the complex anatomy and pathology in the setting of space-occupying lesions, introduce pitfalls that urge caution in the interpretation of abnormal tractography results.<sup>32</sup> The diffusion tensor properties of anatomically and pathologically

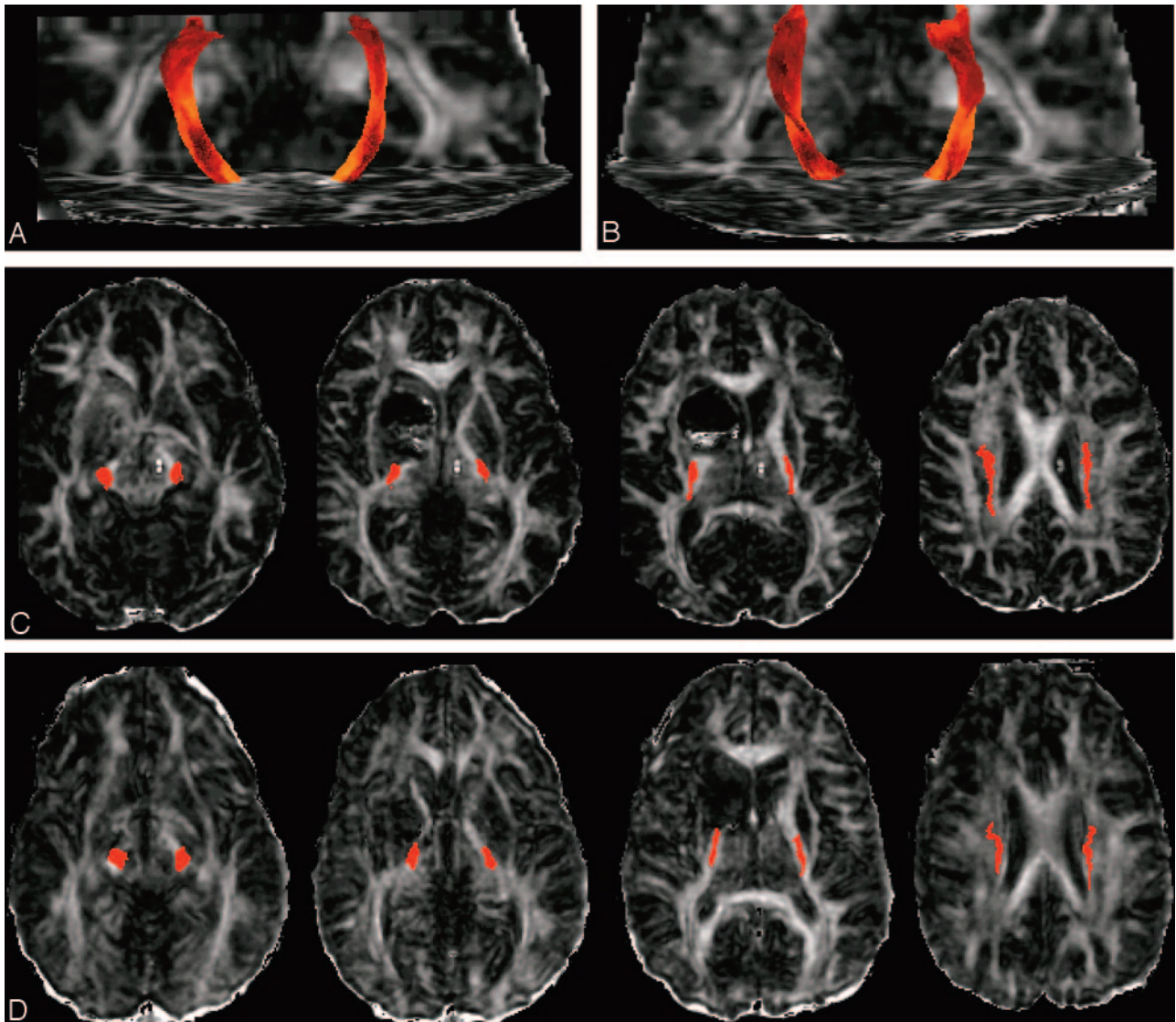


**Fig 14.** Pre- (A) and postoperative (B) tractograms of the corticospinal tracts for patient 6. C and D, The corresponding anatomic locations of the tracts are shown. The tract appears to be preserved postoperatively.

altered tissue are currently not fully understood.<sup>10,11</sup> As noted previously, abnormal trajectories may be either pathologic or technical in origin. For example, the apparent postoperative interruption of the ipsilateral cingulum bundle trajectories in patient 1 (Fig 4B) may reflect actual tract interruption but may rather be due to either incorrect estimation of tract direction resulting from low anisotropy, partial volume effects, or other image artifacts. Whereas the interpretation of abnormal tractograms is difficult, a normal-appearing tractogram should be a strong indication of tract preservation. Continuous WMT connectivity patterns may be useful as a measure of overall tract integrity in the setting of mass lesions; so may the “fiber density index” recently introduced.<sup>33</sup>

On the basis of the tractography results of this study, we have defined several patterns of tract alteration including deviation, interruption, and infiltration. We did not distinguish between edema and tumor because DTI criteria alone do not yet allow this distinction to be made reliably enough to justify distinct terminology.<sup>10,11,32</sup> Whereas the terms “edematous”

and “tumor-infiltrated” might, in some circumstances, be appropriate on the basis of clinical considerations (eg, a T2-hyperintense tract adjacent to a tumor known to be noninfiltrating might reasonably be described as “edematous”), these terms are not DTI-based. An additional pattern, tract degeneration, was not observed in the patients presented here but has been observed previously.<sup>19</sup> Regarding tract deviation, several patterns were observed, including deviation with splaying and/or deformation. Although the definitions introduced here are not perfect (eg, a severely deviated or infiltrated tract might be mistaken for an interrupted one), they represent a reasonable approach, given the current limitations of DTI and tractography.

The tract infiltration pattern was observed in several cases, such as the preoperative ipsilateral corona radiata in patient 4 (Fig 9A). Preservation of tract coherence in regions of low anisotropy suggests conservation of WM organization to some degree. In a recent study correlating fiber-tracking with biopsy results, it was shown that continuous tract trajectories in re-

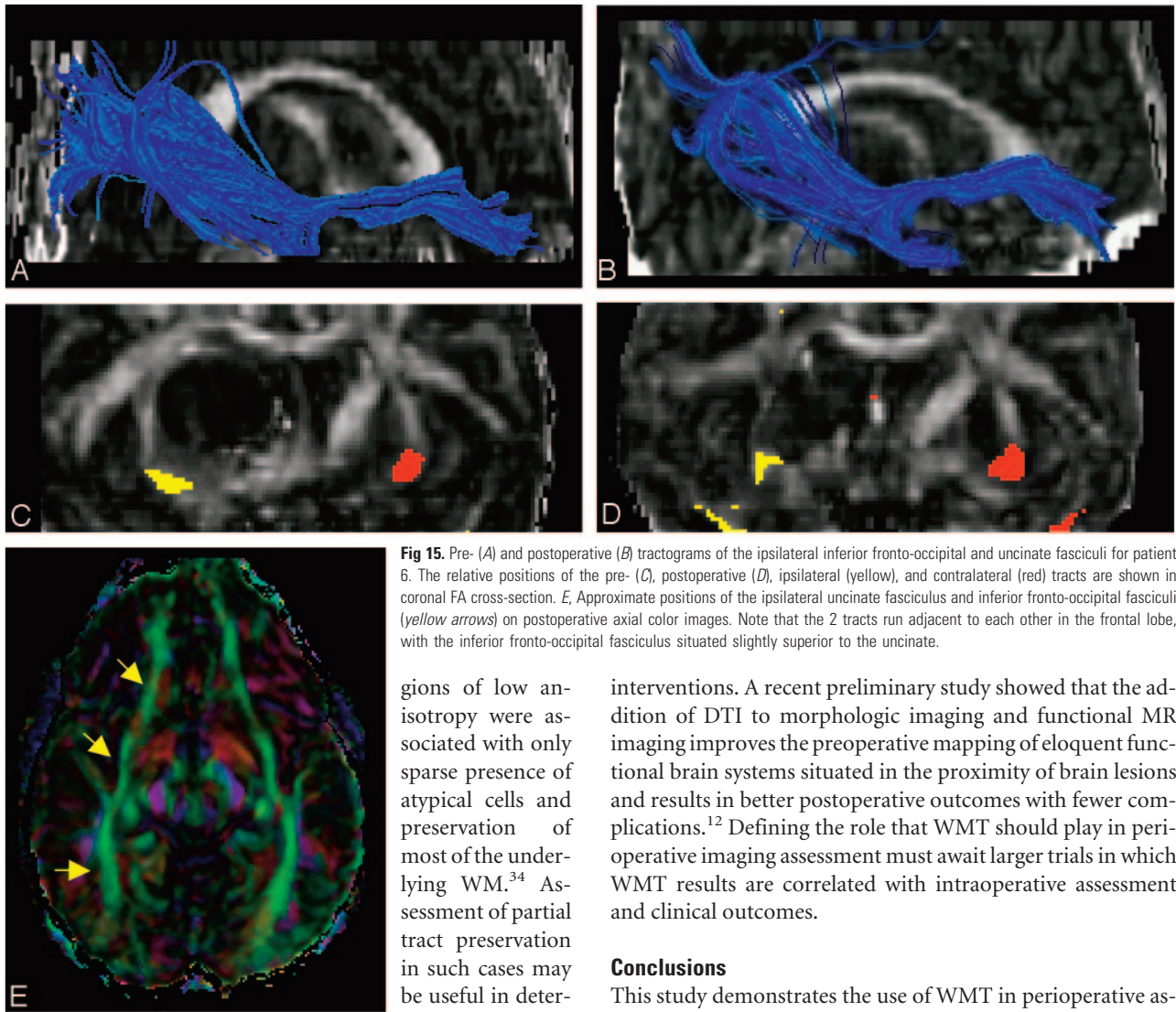


**Fig 15.** Pre- (A) and postoperative (B) tractograms of the ipsilateral inferior fronto-occipital and uncinate fasciculi for patient 6. The relative positions of the pre- (C), postoperative (D), ipsilateral (yellow), and contralateral (red) tracts are shown in coronal FA cross-section. E, Approximate positions of the ipsilateral uncinate fasciculus and inferior fronto-occipital fasciculus (yellow arrows) on postoperative axial color images. Note that the 2 tracts run adjacent to each other in the frontal lobe, with the inferior fronto-occipital fasciculus situated slightly superior to the uncinate.

gions of low anisotropy were associated with only sparse presence of atypical cells and preservation of most of the underlying WM.<sup>34</sup> Assessment of partial tract preservation in such cases may be useful in determining the course

of treatment when eloquent structures are involved.<sup>34</sup>

To our knowledge, this is one of the first studies to use both DTI and WMT to evaluate the effects of surgical resection of tumors and cavernous malformations on the surrounding WM. These techniques potentially provide an important new tool for radiologic assessment before and after neurosurgical

interventions. A recent preliminary study showed that the addition of DTI to morphologic imaging and functional MR imaging improves the preoperative mapping of eloquent functional brain systems situated in the proximity of brain lesions and results in better postoperative outcomes with fewer complications.<sup>12</sup> Defining the role that WMT should play in perioperative imaging assessment must await larger trials in which WMT results are correlated with intraoperative assessment and clinical outcomes.

### Conclusions

This study demonstrates the use of WMT in perioperative assessment of fiber tracts altered by space-occupying lesions and their resection. Examples of several patterns of altered tracts were presented, and a lexicon for discussing such patterns in this and future work was suggested. Future studies with intraoperative correlation and measures of clinical outcome are still required to define the role of WMT in perioperative imaging evaluation.

**Table 2: Lesion effect on the adjacent white matter tracts and tract assessment after surgery**

Patient No.	Tract	Preoperative Assessment Based on Tractography	Postoperative Assessment Based on Tractography
1	Left CB	Deviated and infiltrated	Returns to normal position; locally interrupted
	Left CST	Deviated and deformed	Close to normal
	CC	Interrupted and partially deviated	Reduced deviations/thinned
2	Left CST	Deviated	Normal
	Left IFOF	Locally interrupted	Locally interrupted
3	Left CST	Deviated (with splaying and deformation)	Reduced deviation
4	Right CR	Infiltrated and partially deviated	More normal appearing; no apparent deviation; reduced region of infiltration
	Right CC	Deviated and partially infiltrated	No apparent deviation; reduced region of infiltration
	Right SLF	Deviated and possible infiltration	No apparent deviation or infiltrations of the trunk region
5	Left CST	Deviated	More normal position
6	Right CST	Slightly deviated	Normal
	Right IFOF/UF	Minor deviations with deformation	More normal position

Note:—CB indicates cingulum bundle; CST, cortico-spinal tract; CC, corpus callosum; IFOF, inferior fronto-occipital fasciculus; CR, corona radiata; SLF, superior longitudinal fasciculus; UF, uncinate fasciculus.

## References

1. Conturo TE, Lori NF, Cull TS, et al. **Tracking neuronal fiber pathways in the living human brain.** *Proc Natl Acad Sci U S A* 1999;96:10422–47
2. Basser PJ, Pajevic S, Pierpaoli C, et al. **In vivo fiber tractography using DT-MRI data.** *Magn Reson Med* 2000;44:625–32
3. Mori S, Crain BJ, Chacko VP, et al. **Three-dimensional tracking of axonal projections in the brain by magnetic resonance imaging.** *Ann Neurol* 1999;45:265–69
4. Mori S, van Zijl PC. **Fiber tracking: principles and strategies—a technical review.** *NMR Biomed* 2002;15:468–80
5. Lazar M, Weinstein DM, Tsuruda JS, et al. **White matter tractography using tensor deflection.** *Hum Brain Mapp* 2003;18:306–21
6. Basser PJ, Pierpaoli C. **Microstructural and physiological features of tissues elucidated by quantitative diffusion tensor MRI.** *J Magn Reson B* 1996;111:209–19
7. Wieshmann UC, Symms MR, Parker GJ, et al. **Diffusion-tensor imaging demonstrates deviation of fibres in normal-appearing white matter adjacent to a brain tumour.** *J Neurol Neurosurg Psychiatry* 2000;68:501–03
8. Witwer BP, Moftakhar R, Hasan KM, et al. **Diffusion tensor imaging of white matter tracts in patients with cerebral neoplasm.** *J Neurosurg* 2002;97:568–75
9. Nimsky C, Ganslandt O, Hastreiter P, et al. **Intraoperative diffusion tensor MR imaging: shifting of white matter tracts during neurosurgical procedures—initial experience.** *Radiology* 2005;234:218–25
10. Field AS, Alexander AL, Wu YC, et al. **Diffusion-tensor eigenvector directional color imaging patterns in the evaluation of cerebral white matter tracts altered by tumor.** *J Magn Reson Imaging* 2004;20:555–62
11. Field AS, Alexander AL. **Diffusion tensor imaging in cerebral tumor diagnosis and therapy.** *Top Magn Reson Imaging* 2004;15:315–24
12. Ulmer JL, Salvan CV, Mueller WM, et al. **The role of diffusion tensor imaging in establishing the proximity of tumor borders to functional brain systems: implications for preoperative risk assessments and postoperative outcomes.** *Technol Cancer Res Treat* 2004;3:567–76
13. Holodny AI, Ollenschleger MD, Liu WC, et al. **Identification of the corticospinal tracts achieved using blood-oxygen-level-dependent and diffusion functional MR imaging in patients with brain tumors.** *AJNR Am J Neuroradiol* 2001;22:83–88
14. Mori S, Frederiksen K, van Zijl PC, et al. **Brain white matter anatomy of tumor patients evaluated with diffusion tensor imaging.** *Ann Neurol* 2000;51:377–80
15. Clark CA, Barrick TR, Murphy MM, et al. **White matter fiber tracking in patients with space-occupying lesions of the brain: a new technique for neurosurgical planning?** *Neuroimage* 2003;20:1601–08
16. Henry RG, Berman JI, Nagarajan SS, et al. **Subcortical pathways serving cortical language sites: initial experience with diffusion tensor imaging fiber tracking combined with intraoperative language mapping.** *Neuroimage* 2004;21:616–22
17. Berman JI, Berger MS, Mukherjee P, et al. **Diffusion-tensor imaging-guided tracking of fibers of the pyramidal tract combined with intraoperative cortical stimulation mapping in patients with gliomas.** *J Neurosurg* 2004;101:66–72
18. Alexander AL, Badie B, Field AS. **Diffusion Tensor MRI Depicts White Matter Reorganization After Surgery: Proceedings of 11th International Society for Magnetic Resonance in Medicine (ISMRM) Scientific Meeting, Toronto, Ontario, Canada, July 10–16, 2003:399**
19. Laundre BJ, Jellison BJ, Badie B, et al. **Diffusion tensor imaging of the corticospinal tract before and after mass resection as correlated with clinical motor findings: preliminary data.** *AJNR Am J Neuroradiol* 2005;26:791–96
20. Catani M, Howard RJ, Pajevic S, et al. **Virtual in vivo interactive dissection of white matter fasciculi in the human brain.** *Neuroimage* 2002;17:77–94
21. Lazar M, Field AS, Lee JH, et al. **Lateral Asymmetry of Superior Longitudinal Fasciculus: A White Matter Tractography Study—Proceedings of 12th International Society for Magnetic Resonance in Medicine (ISMRM) Scientific Meeting, Kyoto, Japan, May 15–22, 2004**
22. Yu CS, Li KC, Xuan Y, et al. **Diffusion tensor tractography in patients with cerebral tumors: a helpful technique for neurosurgical planning and postoperative assessment.** *Eur J Radiol* 2005;56:197–204
23. Nimsky C, Ganslandt O, Hastreiter P, et al. **Preoperative and intraoperative diffusion tensor imaging-based fiber tracking in glioma surgery.** *Neurosurgery* 2005;56:130–37
24. Hammerstad JP. **Strength and reflexes.** In: Goetz CG. *Textbook of Clinical Neurology*, 2nd ed. Philadelphia, Pa: Elsevier Science; 2003:225–65
25. Woods RP, Grafton ST, Holmes CJ, et al. **Automated image registration. I. General methods and intrasubject, intramodality validation.** *J Comput Assist Tomogr* 1998;22:141:154
26. Pajevic S, Pierpaoli C. **Color schemes to represent the orientation of anisotropic tissues from diffusion tensor data: application to white matter fiber tract mapping in the human brain.** *Magn Reson Med* 1999;42:526–40
27. Anderson AW. **Theoretical analysis of the effects of noise on diffusion tensor imaging.** *Magn Reson Med* 2001;46:1174–88
28. Lazar M, Alexander AL. **An error analysis of white matter tractography methods: synthetic diffusion tensor field simulations.** *Neuroimage* 2003;20:1140–53
29. Alexander AL, Hasan KM, Lazar M, et al. **Analysis of partial volume effects in diffusion tensor MRI.** *Magn Reson Med* 2001;45:770–80
30. Frank LR. **Characterization of anisotropy in high angular resolution diffusion-weighted MRI.** *Magn Reson Med* 2002;47:1083–99
31. Tuch DS, Reese TG, Wiegell MR, et al. **Diffusion MRI of complex neural architecture.** *Neuron* 2003;40:885–95
32. Field AS. **Diffusion tensor imaging at the crossroads: fiber tracking meets tissue characterization in brain tumors.** *AJNR Am J Neuroradiol* 2005;26:2168–69
33. Roberts TPL, Liu F, Kassner A, et al. **Fiber density index correlates with reduced fractional anisotropy in white matter of patients with glioblastoma.** *AJNR Am J Neuroradiol* 2005;26:2183–86
34. Akai H, Mori H, Aoki S, et al. **Diffusion tensor tractography of gliomatosis cerebri: fiber tracking through the tumor.** *J Comput Assist Tomogr* 2005;29:127–29